Waste-to-hydrogen via CO_2/steam-enhanced gasification of spent coffee ground

Juliana Petrocchi Rodrigues [a], Grace F. Ghesti [b,*], Edgar A. Silveira [c,*], Giulia Cruz Lamas [c], Ricardo Ferreira [d], M. Costa [d,†]

[a] Faculty of Gama, University of Brasília, Brasília, DF 70910-900, Brazil
[b] Laboratory of Brewing Bioprocesses and Catalysis to Renewable Energy, Chemistry Institute, University of Brasilia, Brasilia DF 70910-900, Brazil
[c] Mechanical Sciences Graduate Program, University of Brasília, Brasília DF, Brazil
[d] IDMEC, Mechanical Engineering Department, Instituto Superior Técnico, Universidade de Lisboa, Lisboa, Portugal

ARTICLE INFO

ABSTRACT

This paper evaluated steam and CO_2-enhanced gasification of spent coffee ground (SCG) biomass, including energy and exergy aspects focusing on hydrogen production. The waste-to-hydrogen (WTH) conversion was performed via gasification (1000 °C) with a drop-tube-reactor investigating six different steam to biomass (SBR of 0.5, 0.8 and 1.2) and CO_2 to biomass (CO_2BR 0.09, 0.18 and 0.27) ratios. The syngas production indicated clear improvement against O_2/N_2 with an H_2 yield increase up to 69.21% and 18.32% for steam and CO_2 mediums. The energy and exergy analysis points out the 0.8 SBR as the optimum condition with 210% CGE and 48.05% exergy efficiency for H_2 production. As a strategy for carbon capture and usage, the medium with 0.27 CO_2BR provided a 28.52% exergy efficiency for H_2 production and reduced soot formation, showing a potential gasification medium for SCG. Results encourage waste-to-hydrogen prospection within circular economy principles, boosting circular economy principles in urban districts.

1. Introduction

An enhanced amount of greenhouse gas (GHG) released from energy production units and industrial sectors using fossil fuels is a significant cause of global warming (Detchusananard et al., 2018). Environmental issues have raised global awareness, reflected in research on carbon mitigation, conversion, and storage (Prasertcharoensuk et al., 2021; Silveira et al., 2022a). The focus on sustainable goals permeates companies' responsibility for their processes and disposal of products, pursuing strategies that demonstrate their concern for environmental sustainability (Deutsch et al., 2022). The replacement of the model based on the refining of fossil sources for a model of biorefineries of organic material residues indicates a great effort in carbon management and mitigation of global warming (Cséfalvay and Horváth, 2018; Santanna et al., 2020).

Previous studies provided insights into the use of unavoidable and carbon-neutral residues produced in urban districts (Evaristo et al., 2021; Ghesti et al., 2022; Menezes et al., 2022), promoting the biorefinery perception and urban symbiosis, leveraging high-value-added products that increase the overall financial system and the move to a circular concept in urban areas (Silveira et al., 2022c, 2022b). In this context, the environmental concerns because of the disposal of SCG, summed

to its valuable properties (high carbon content, high heating value, low ash, and negligible sulfur content, encourage this waste as an alternative fuel source (Atabani et al., 2022a; Kibret et al., 2021).

Coffee beans are produced in over 46 countries, offering about 8.60 million tons worldwide (Dang and Nguyen, 2019). Brazil (30%), Vietnam (19%), and Columbia (9%) are the primary producers and exporters of coffee beans (Dang and Nguyen, 2019). Coffee is an agro-based product, widely consumed as a beverage drink and the 2nd largest commodity after petroleum and its derivatives (Atabani et al., 2022b; Rajesh Banu et al., 2021). Consequently, the coffee industry generates vast organic waste, where the spent coffee ground (SCG) is the most valuable (McNutt and He, 2019).

SCG amounts to approximately 40% of the total coffee bean mass (Efthymiopoulos et al., 2018). Around 650 kg of SCG is generated from 1 ton of coffee beans, representing an average annual production of 8 million tonnes (Colantoni et al., 2021). It is estimated that 93% of SCG is directly forwarded to landfills without proper treatment, promoting environmental threats as GHGs emissions (mainly CO_2 and CH_4) (Atabani et al., 2022a).

Hydrogen (H_2), recognized as one of the cleanest energy vectors, can be produced from lignocellulosic biomass, a promising raw material for achieving a sustainable bioeconomy (Moreira et al., 2021; Rajesh

Index Summary

β	biomass correlation factor
CCE	carbon conversion efficiency
CEI	carbon enhancement index
CGE	cold gas efficiency
CO	carbon monoxide
CO_2	carbon dioxide
DTG	thermogravimetric derivative
$Ex_{biomass}$	exergy of biomass
Ex^{ch}	chemical exergy
Ex^{ki}	kinetic exergy
Ex^{ph}	physical exergy
Ex^{po}	potential exergy
$ex_{H_2}^{ch}$	standard chemical exergy
Ex_{H2}	exergy of hydrogen
h	specific enthalpy
h_0	specific enthalpy
LHV	lower heating value
$\dot{m}_{bio}$	biomass feeding rate
n	molar yield
η_{H_2}	exergy efficiency of hydrogen
Q_{syngas}	syngas flow rate
r_i	mole fraction
s	specific entropy
s_0	specific entropy at T_0
SCG	spent coffee ground
SEM	Scanning Electron Microscope
γ_{syngas}	syngas yield
T	temperature
t	time
WTH	waste-to-hydrogen
$x_{carbon, i}$	carbon molar fraction
y_{carbon}	feedstock carbon mass fraction
y_{CO} or y_{H_2}	CO or H_2 percentage in syngas

Banu et al., 2021). The increasing projection of H_2 demand is around 17% per annum in the coming years from a current baseline of 55 million tonnes/year due to its wide range of applications in chemical (57%), petroleum (37%), and agrochemical (6%) industries (Ashik et al., 2015; Prasertcharoensuk et al., 2021). The previous review has focused on WTH technologies, the associated environmental impacts, and economic and social aspects (Wijayasekera et al., 2022). Regarding the thermochemical WTH routes, past work pointed out that gasification and pyrolysis are the two primary processes (Wijayasekera et al., 2022).

The gasification process converts any carbon-based raw material into synthetic gas (Midilli et al., 2021; Santanna et al., 2021). Gasification evolves a partial oxidation reaction of organic substances at a temperature range of 900–1500 °C. The process is considered the most cost-effective and efficient method to produce hydrogen that can replace the steam reforming of fossil fuels (Prasertcharoensuk et al., 2021). Furthermore, gasification can occur in different atmospheres, e.g., O_2, depleted air, CO_2, steam, or mixtures of these compounds (Adánez-Rubio et al., 2020). Table 1 summarizes previous literature on lignocellulosic biomass focusing on WTH production by applying different gasification mediums.

As an alternative for energy generation from residues of the coffee harvest, gasification was extensively reviewed by (Mendoza Martinez et al., 2021a), which shows few studies focusing on the coffee pulp (Parascanu et al., 2017; Torres et al., 2019), husks (Couto et al., 2013; de Oliveira et al., 2018; George et al., 2019; Ismail et al., 2016), and SCG (Pacioni et al., 2016).

In addition, recent studies on SCG gasification described the kinetic modeling of CO_2 gasification for SCG biochar (Pacioni et al., 2021), the

two-step gasification of SCG biochar for hydrogen-rich gas production (Cay et al., 2019), the thermal behavior and product yield of SCG steam catalytic gasification (Chaiklangmuang et al., 2015), and the steam and CO_2 gasification under different concentrations (Kibret et al., 2021). However, due to the limited studies that focus on energy generation from coffee production chain residues, only partial information describing the thermochemical process implementations on SCG residues is available (Mendoza Martinez et al., 2021b).

Furthermore, the studies that attempt to produce syngas from SCG by different gasification agents are still limited in the current literature. Thus, considering the perspective of WTH from SCG and the limited literature, a comprehensive experimental assessment was performed for steam/CO_2-enhanced gasification processes assessing energy and exergy aspects focusing on H_2 production from SCG.

2. Material and methods

2.1. SCG feedstock

The SCG material comprises Arabica coffee species supplied by local coffee brands (Café Export) from Brasília, Brazil. Before gasification experiments and chemical characterization, the raw SCG residues were oven-dried until dry (105 ± 1 °C for 24 h), ground and sieved (using a mechanical sieve shaker with 60 mesh sieve) to sizes between 177 μm (80mesh) and 250 μm (60mesh). The main chemical properties of the SCG biomass feedstock are shown in Table 2.

The following methods were applied for the ultimate analysis (ASTM E777/2008 e E778/2008) and proximate analysis (ASTM D 5142–09 for volatile matter, TAPPI T211 om-93 standard for ashes (Miranda et al., 2020)) of raw SCG samples. Other components were determined using a Shimadzu X-ray Fluorescence (XRF) spectrometer (model EDX 720) with a Rhodium tube as an X-ray source (Evaristo et al., 2021). The thermogravimetric analysis (TG) was evaluated for 5 ± 0.1 mg with Shimadzu DT-60 TGA equipment in an inert atmosphere with a 20 °C.min^{-1} heating rate from room temperature until 800 °C (Galvão et al., 2020). The experiments were performed in duplicate to verify reproducibility. The SEM images (SHIMADZU equipment with 400 and 1000X) and the thermogravimetric analysis (TG and its derivative, DTG) are illustrated in Fig. 1.

2.2. Gasification

The proposed framework of the study is illustrated in Fig. 2. The gasification system was applied and validated in previous works (Evaristo et al., 2021; Ferreira et al., 2021; Ghesti et al., 2022). First, a twin-screw volumetric feeder poured the SCG residues at a 0.03 kg.h^{-1} feeding rate to the water-cooled injector. Next, the biomass particles (and the carrier gas N_2) are injected into a vertical nonporous mullite tube within the vertical electrically heated drop tube reactor (DTR–12 kW). The wall temperature of the mullite tube (1750 mm in length and a 40 mm inner diameter) was monitored by three type-K thermocouples. The wall temperature was maintained at 1000 °C and particles injected from the top of the DTR typically experience heating rates of ~10^5 K.s^{-1} (Adánez-Rubio et al., 2020). Finally, the SCG was injected from the top of the DTR with a constant wall temperature of 1000 °C during gasification essays (Ferreiro et al., 2020).

A concentric passage between the mullite tube and the injector inserted the three distinct gasification mediums (O_2/N_2, $O_2/CO_2/N_2$ and $O_2/H_2O/N_2$) streams with an inlet gas flow of 1 dm^3.min^{-1} (N_2 used to balance) (Adánez-Rubio et al., 2020). Therefore, ensuring the homogeneous mixture of N_2, O_2 and steam, or CO_2, into the tube for each specific experiment condition. A steam generator (evaporator at 2 bar pressure) delivered the moisture. Meanwhile, the CO_2 and O_2 were supplied from pressurized containers. The Steam-to-biomass ratio (SBR) and CO_2-to-biomass ratio (CO$_2$BR) were defined as the mass flow rate of the injected medium (g.h^{-1}) divided by that of the biomass feed rate (g.h^{-1})

Table 1
Summary of lignocellulosic biomass focusing on WTH production.

Year	Feedstock	Laboratory scale Gasification process conditions	Performance indicators	Ref.
2016	SCG	**TGA** **Temperature:** 650–850 °C **Reaction time:** 2 h **Medium:** argon/steam mixture Steam concentration 5–30 vol%	Syngas composition LHV [a], HHV [b]	(Pacioni et al., 2016)
2021	Wheat straw	**Temperature:** 700 °C **Reaction time:** 30 min **Medium:** supercritical water	CGE [c], LHV H_2 yield, H_2 efficiency	(Wang et al., 2021)
2021	Waste furniture	**Temperature:** 800 °C **Reaction time:** – **Medium:** steam **Catalyst:** rice husk biochar	Syngas composition Gas yield H_2 content	(Farooq et al., 2021)
2021	Cornstalk	**Temperature:** 750 °C **Reaction time:** – **Medium:** excess oxygen ratio – 0.2 KNO_3 content: 8% (w/w)	H_2 efficiency H_2 yield	(Qin et al., 2021)
2021	Banana peel, Japanese cedar wood, and rice husk	**Temperature:** 650–850 °C **Reaction time:** 120 min **Medium:** steam **Catalyst:** K (alkaline earth metal) **Pressure:** 1 atm	Gas yield CCE [d]	(Anniwaer et al., 2021)
2020	Palm empty fruit bunch	**Temperature:** 700 °C **Medium:** steam Steam to feedstock ratio: 2 **Catalyst:** commercial Zeolite **Pressure:** 1 atm CaO to feedstock ratio: 1	Syngas composition H_2 yield H_2 efficiency	(Inayat et al., 2020)
2021	Brewers' spent grains	**Drop tube reactor** **Temperature:** 1000 °C **Reaction time:** 30 min **Medium:** O_2/N_2 $O_2/CO_2/N_2$ $O_2/H_2O/N_2$	Syngas composition CGE, CCE, LHV H_2 exergy H_2 efficiency	(Evaristo et al., 2021)
2021	SCG	**Semi-fluidized bed reactor** **Temperature:** 700–900 °C **Reaction time:** 30 min **Medium:** $O_2/H_2O/N_2$ S/B molar ratio: 0.14, 0.27, 0.4, 0.53 **Medium:** $O_2/CO_2/N_2$ CO_2/B molar ratio: 0.11, 0.14, 0.17, 0.21	Syngas composition Carbon conversion, CGE, LHV H_2/CO	(Kibret et al., 2021)
This work	SCG	**Drop tube reactor** **Temperature:** 1000 °C **Residence time:** 2–3 s **Medium:** O_2/N_2 (λ=0.4) **Medium:** $O_2/CO_2/N_2$ CO_2/biomass:0.09, 0.18 and 0.27 **Medium:** $O_2/H_2O/N_2$ Steam/biomass: 0.5, 0.8 and 1.2	Syngas composition CCE, CGE, LHV and H_2/CO Soot and char formation H_2 exergy H_2 efficiency	study

[a] LHV lower heating value
[b] HHV – higher heating value
[c] CGE – cold gas efficiency
[d] CCE – carbon conversion efficiency.

(Bach et al., 2019). The distinct inlet concentrations were controlled by flow meters within the gas line.

A particle collection system composed of two cyclones (able to capture char particles>10 μm and particles soot and char particles <10 μm) was positioned at the bottom of the DTR. The syngas composition was measured using a paramagnetic pressure analyzer for O_2 and a non-dispersive infrared analyzer for CO_2 and CO. The remaining gasses were identified by a gas chromatograph Clarus 500 (Adánez-Rubio et al., 2020). All experiments had a duration of around 10 min, contemplating the temperature stabilization of the reactor, the time the SCG biomass (60–80mesh) dropped freely within the DTR (~2–3 s), and their solid residues (soot and char) and producer gas collection. The gasification operational conditions based on previous studies (Adánez-Rubio et al., 2020; Evaristo et al., 2021; Ferreiro et al., 2020) are describe in Table 3.

Understanding the primary reactions of the thermochemical process helps to have some perspective on the process and gives a chance to improve the process and the system (Kibret et al., 2021). Equation (01) describes the thermal conversion of biomass during gasification.

$$CH_{1.5}N_{0.04}O_{0.5} \rightarrow CO + CO_2 + CH_4 + H_2 + C_2H_4 + Char + Tar \quad (1)$$
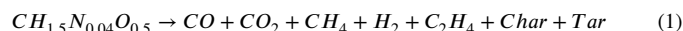
Here, SCG (represented by its chemical formula) passes through two stages concerning the fast pyrolytic process followed by char gasification and tar decomposition (Kibret et al., 2021). The main gasification reactions that progressed during the thermal conversion are summarized in Table 4.

The following energy performance indicators were determined to evaluate the gasification processes: the lower heating value of the syngas (LHV_{syngas}), syngas yield (γ_{syngas}), carbon conversion efficiency (CCE),

Table 2

The proximate, ultimate analysis, EDX and energy parameters for SCG raw material (Evaristo et al., 2021).

Feedstock	SCG
Proximate analysis (wt%)	
Ash	1.67
Fixed carbon	17.71
Volatile Matter	80.62
Moisture	5.47
Ultimate analysis (wt%) [a]	
C	57.74
H	7.22
N	2.39
O [b]	38.65
Formula	$CH_{1.5}N_{0.04}O_{0.5}$
EDX (mg. $kg_{biomass}^{-1}$)	
Ca	791
K	4201
Mg	696
Na	122
P	123
Si	65
Energy parameters (MJ. kg^{-1})	
HHV [b]	21.04
LHV [c]	19.45

[a] Dry basis.
[b] By difference O = 100 − (C + H + N).
[c] $LHV = HHV - 21.97 \times H$.

and cold gas efficiency (CGE) (Adánez-Rubio et al., 2020). Primarily, performing an exergy analysis provides meaningful and superior information than energy analysis. Therefore, the exergy of H_2-production and its exergy efficiency were assessed (Hu et al., 2021; Parvez et al., 2016; Zhang et al., 2019b, 2019a).

2.3. Energy analysis

The LHV_{syngas} (Eq. (02)) was determined as a function of the mole fraction (r_i) and lower heating value (LHV_i) of a constituent $i = H_2$,
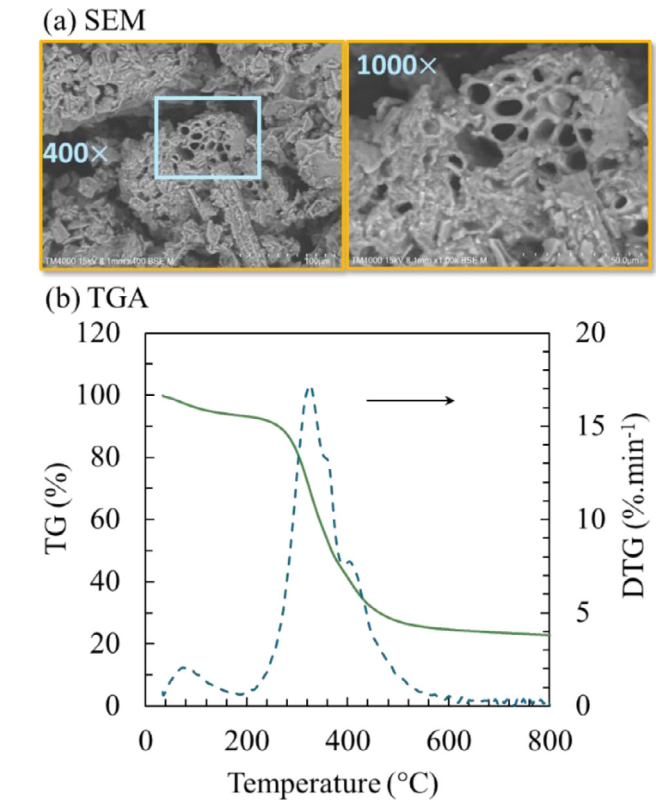

Fig. 1. SEM characterization and thermogravimetric (TG and DTG) profiles of raw SCG feedstock.

CH_4, and CO of the dry fuel gas (Waldheim and Nilsson, 2001).

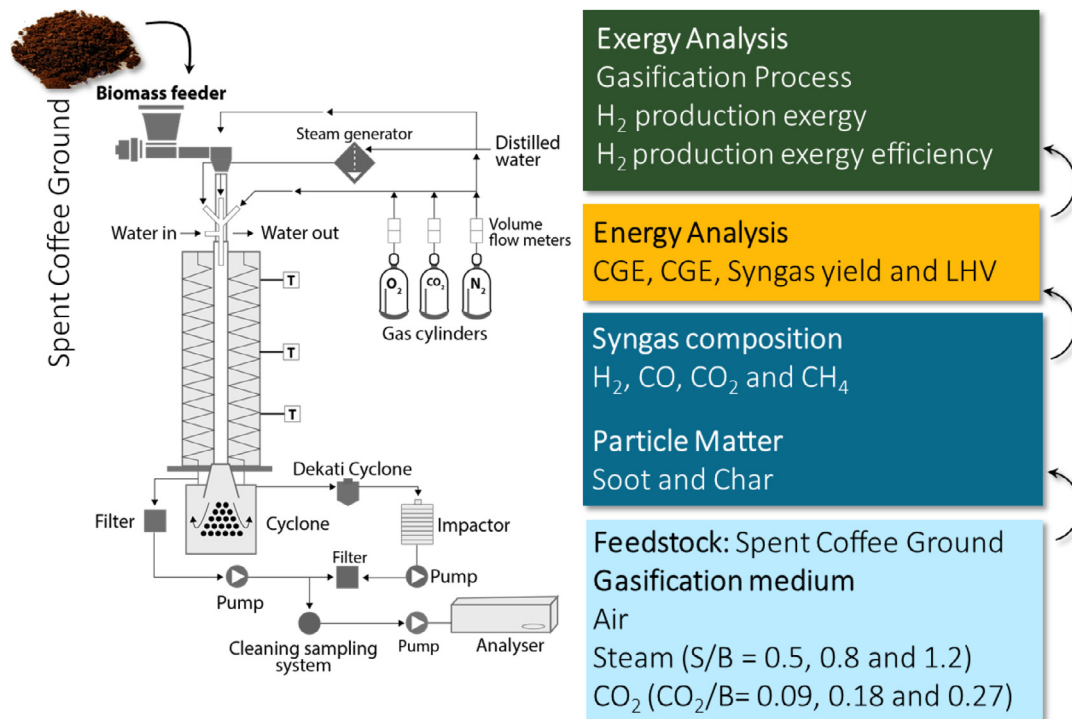$$LHV_{syngas} = \sum r_i LHV_i \qquad (2)$$

Fig. 2. Gasification apparatus (Adánez-Rubio et al., 2020) and proposed framework.

Table 3

Gasification operational process for the drop tube reactor system (Fig. 2).

Parameters	Values
Biomass feed rate	30 g.h^{-1}
Gasification temperature	1000 °C
Particle residence time	~2–3 s
Atmosphere (stream flow rate)	
CO_2	2.82, 5.40, 8 g.h^{-1}
H_2O	15, 25, and 35 g.h^{-1}

Table 4

Main gasification reactions (Reyes et al., 2021; Tang et al., 2022; Vikram et al., 2022).

	Reaction name	Equation	ΔH (kJ. mol^{-1}) [a]
R_1	Partial oxidation	$C + 1/2O_2 \rightarrow CO$	-111
R_2	Char combustion	$C + O_2 \rightarrow CO_2$	-394
R_3	Boudouard reaction	$C + CO_2 \leftrightarrow 2CO$	172
R_4	Char reforming	$C + H_2O \leftrightarrow CO + H_2$	131
R_5	Water gas-shift	$CO + H_2O \leftrightarrow CO_2 + H_2$	-41
R_6	Methanation	$C + 2H_2 \leftrightarrow CH_4$	-75
R_7	Steam-methane reforming	$CH_4 + H_2O \leftrightarrow CO + 3H_2$	206

[a] Heat of reaction.

The syngas yield (γ_{syngas}) was defined by Eq. (03) as the amount of H$_2$, and CO generated during the process of gasification (mol syngas. kg$_{biomass}$$^{-1}$). The γ_{syngas} was calculated in terms of the biomass feeding rate $\dot{m}_{bio}$ in kg.h^{-1} (Table 3), the Q_{syngas} is the syngas flow rate (Nm^3.h^{-1}) and y_i is the gas molar fraction of CO and H$_2$ (Adánez-Rubio et al., 2020)

$$\gamma_{syngas} = \frac{(Q_{syngas} \times y_{CO}) + (Q_{syngas} \times y_{H_2})}{\dot{m}_{bio}}. \tag{3}$$

The cold gas efficiency (CGE) was defined as Eq. (04) (Costa et al., 2021; Lamas et al., 2022)

$$CGE = \frac{Q_{syngas} \times LHV_{syngas}}{\dot{m}_{bio} \times LHV_{biomass}}, \tag{4}$$

and carbon conversion efficiency (CCE) as Eq. (05)

$$CCE = \frac{Q_{syngas} \times \sum_i^n x_{carbon, i}}{\dot{m}_{bio} \times y_{carbon}}. \tag{5}$$

Here the $LHV_{biomass}$ (MJ. kg^{-1}) and the carbon mass fraction y_{carbon} are values from (Table 2) and the molar fraction of carbon (x_{carbon}) includes the carbon content of CO, CO$_2$, and CH$_4$ (producer gas products) (Adánez-Rubio et al., 2020; Chen et al., 2013).

2.4. Exergy analysis

The exergy efficiency (η_{H_2}) of H$_2$ production was applied as a gasification performance indicator to compare the different gasification atmospheres (Parvez et al., 2016; Xiang et al., 2021; Zhang et al., 2019a, 2019b). The (η_{H_2}) can be defined by Eq. (06) (Zhang et al., 2019a, 2012) as

$$\eta_{H_2} = \frac{Ex_{H2}}{Ex_{bio}} \times 100\%. \tag{6}$$

The exergy of hydrogen (Ex_{H_2}) in kJ. kg^{-1}, described by Eq. (07), includes only two forms since the potential (Ex^{po}) exergy and the kinetic (Ex^{ki}), which are minimal parts of the total exergy, are neglected (Zhang et al., 2019b, 2015), resulting in

$$Ex_{H_2} = Ex^{ch} + Ex^{ph}. \tag{7}$$

The chemical (Ex^{ch}) exergy was determined through Eq. (08) based on the molar yield (n_{H_2} in mol. kg^{-1}) and the standard chemical exergy ($ex^{ch}_{H_2}$=236,100 kJ. kmol^{-1}) of H$_2$ (Zhang et al., 2019a, 2012).

$$Ex^{ch} = n_{H_2} \times ex^{ch}_{H_2} \tag{8}$$

Meanwhile, the physical (Ex^{ph}) exergy of H$_2$ (kJ. kg^{-1}) was calculated with Eq. (09), where h and h_0 are the specific enthalpy of H$_2$ at arbitrary temperatures (kJ. kmol^{-1}) and in the environment (7926 kJ. kmol^{-1}); s and s_0 the specific entropy of H$_2$ at arbitrary temperatures (kJ. kmol^{-1}K^{-1}) and in the environment (107.71 kJ. kmol^{-1}K^{-1}); T_0 the environmental temperature (298.15 K).

$$Ex^{ph} = n_{H_2} \times \left[(h - h_0) - T_0 \times (s - s_0) \right] \tag{9}$$

The chemical exergy of the biomass feedstock $Ex_{biomass} = \beta \times LHV_{biomass}$ is described by Eq. (10) and can be obtained as a function of the correlation factor β (Evaristo et al., 2021), the LHV of raw biomass (kJ. kg^{-1}) and the weight fraction (%) of biomass feedstock in terms of carbon (C), hydrogen (H), oxygen (O), and nitrogen (N) from Table 2.

$$\beta = \frac{1.044 + 0.0160 \times H/C - 0.3493 \times O/C(1 + 0.0531 \times H/C) + 0.0493 \times N/C}{1 - 0.4124 \times O/C} \tag{10}$$

3. Results and discussions

3.1. Effects of CO$_2$-to-Biomass ratio (CO$_2$BR)

The gasification process is complex and can be influenced by many operational conditions and factors, such as reactor type, process temperature and medium, feedstock, particle size and catalytic effects. Therefore, it is worth noting that all the factors evolved with the process analysis must be similar for competing results on the product gas composition with different works; otherwise, the comparison may be voided (Bach et al., 2019). The present investigation related the gas composition, energy and exergy performance indicators with the temperature of the gasification reactor (not the single biomass particle wich evolves heat and mass transfer mechanisms). In addition, it is worth noting that the obtained results represent the gasification process in DTR conditions and not entrained flow.

Fig. 3(a) shows the composition of the product gas (H$_2$, CO, CO$_2$, and CH$_4$ calculated using an N$_2$-free basis) for O$_2$/N$_2$ (blue region) and CO$_2$-enhanced gasification (O$_2$/CO$_2$/N$_2$) considering three CO$_2$BR (0.009, 0.18 and 0.27).

When the CO$_2$BR rises from 0.09 to 0.27, the CH$_4$ and CO$_2$ contents decrease (from 8.98 to 7.08 vol% and 32.81 to 20.70 vol%, respectively). Meanwhile, the CO content shows only a marginal change from 0.09 to 0.18 CO$_2$BR and increased to 45.62 vol% for 0.27 CO$_2$BR. Regarding the lowest CO$_2$BR (0.09), the producer gas composition did not evidence a pronounced difference from O$_2$/N$_2$ medium, with a slight reduction of H$_2$, CH$_4$ and CO$_2$ and increased CO vol% (Fig. 3(a)). A maximum H$_2$/CO ratio (0.83) was obtained for 0.18 CO$_2$BR, and no pronounced difference in H$_2$/CO was observed for other CO$_2$BR compared to O$_2$/N$_2$ (Fig. 3(c)).

Compared to 0.18 CO$_2$BR, the relative concentration of CO increased, and the H$_2$ decreased for 0.27 CO$_2$BR. This behavior might be related to the more favorable Boudouard reaction (R_3) than water-shift gas (R_5) for higher gasification temperature with CO$_2$ medium (Kibret et al., 2021). The effect of the CO$_2$ medium on the improvement of CO yield and reduction of H$_2$ yield was as expected and in line with previous works (Butterman and Castaldi, 2007; Kibret et al., 2021). Compared to O$_2$/N$_2$, no pronounced difference in the γ_{syngas} was reported for 0.09 CO$_2$BR, followed by an upward trend (from 57.58 to 78.03 mol$_{syngas}$. kg$_{biomass}$$^{-1}$) with increasing CO$_2$BR (Fig. 3(c)).
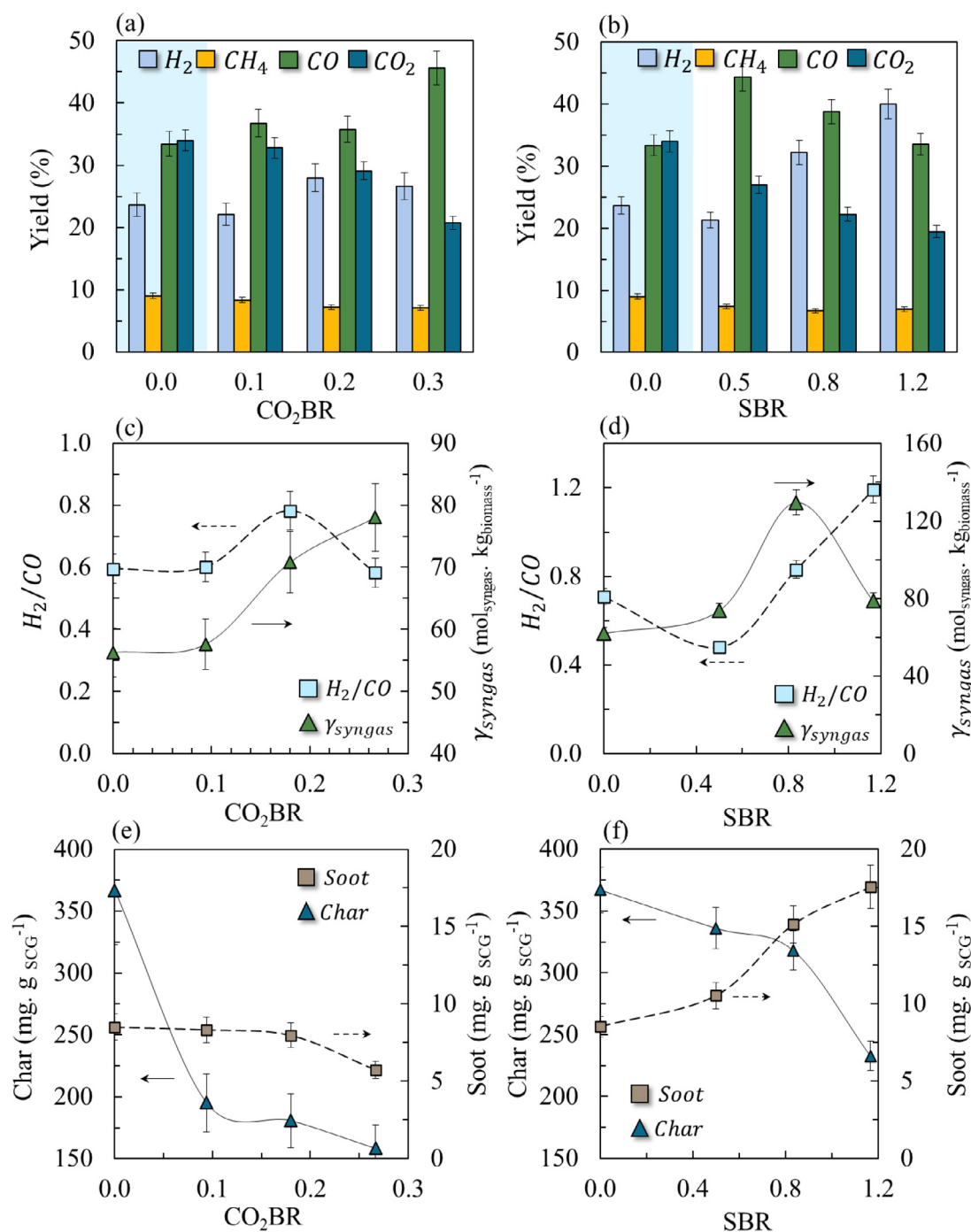
Fig. 3. Producer gas composition (H_2, CO, CO_2, and CH_4) for (a) CO_2BR (0.09, 0.18 and 0.27) and (b) SBR (0.5, 0.8 and 1.2). Blue region designated O_2/N_2. H_2/CO ratio and syngas yield (γ_{syngas}) for (c) CO_2BR (0.09, 0.18 and 0.27) and (d) SBR (0.5, 0.8 and 1.2). Soot and char formation mg. g_{SCG}^{-1} for (e) CO_2BR (0.09, 0.18 and 0.27) and (f) SBR (0.5, 0.8 and 1.2).

Fig. 3(e) shows the soot and char formed through the experiments as a function of the CO_2BR. During the gasification, adding CO_2 significantly reduced char formation to 56.85% (0.27 CO_2BR) less char than O_2/N_2 medium. The downward trend of char formation with CO_2BR increasing is in line with previous SCG gasification on DTR results (Evaristo et al., 2021). Soot formation under 0.09 and 0.18 CO_2BR presented a minimal difference from O_2/N_2 medium, followed by a reduction for 0.027 CO_2BR, achieving 32.69% less soot formation.

3.2. Effects of steam-to-biomass ratio (SBR)

Fig. 3(b) indicates a steady increase in H_2 formation (up to 40%) with increasing SBR. Meanwhile, a decrease in CH_4 (related to reaction R_7), CO (reaction R_5 is enhanced at a higher steam flow rate) and CO_2 (related to R_3) were evidenced. Kibret et al. (2021) investigated SCG gasification in a previous study showing an upward trend for H_2, while CH_4, CO and CO_2 vol% showed a decrease with increasing SBR, in line with Fig. 3. Kibret et al. (2021) reported a growing trend for CO
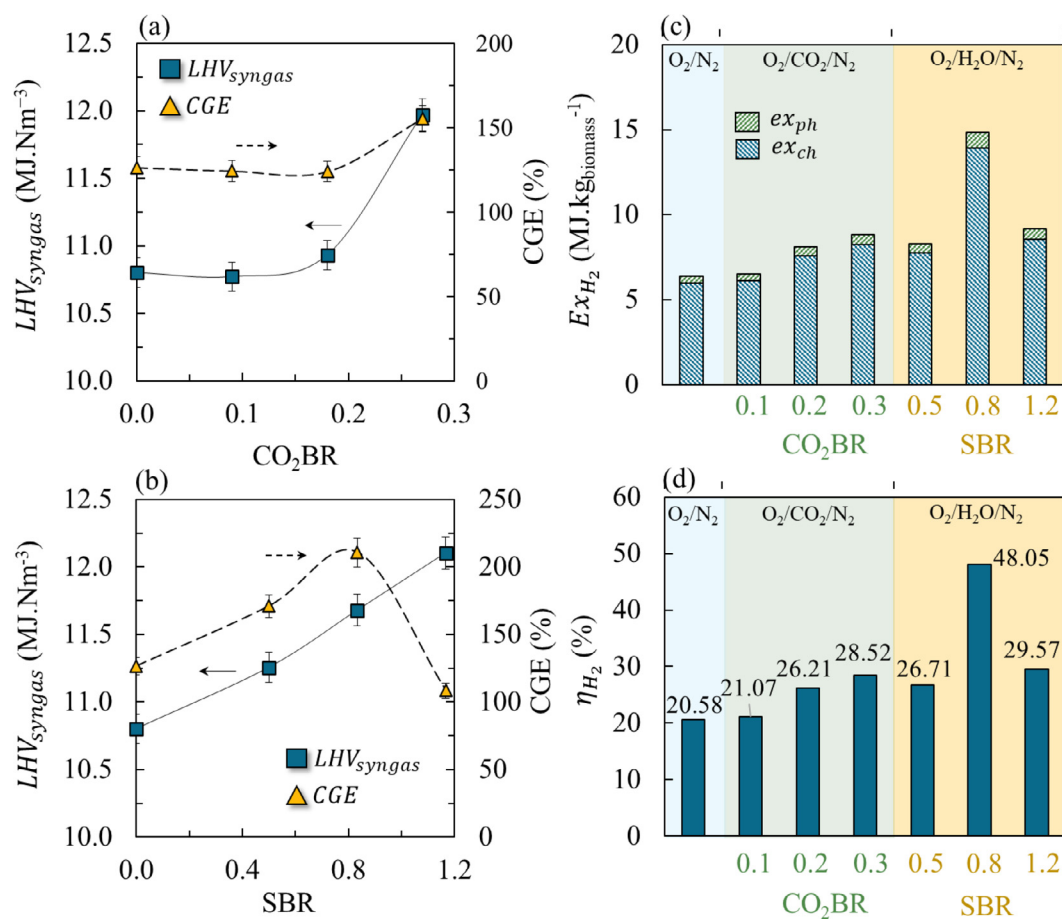
Fig. 4. HV_{syngas} and CGE for CO_2BR (a) and SBR (b). (c) H_2-exergy (Ex_{H_2}) and (d) H_2-exergy efficiency (η_{H_2}) as a function CO_2BR (0.09, 0.18 and 0.27) and SBR (0.5, 0.8 and 1.2). Blue region designated O_2/N_2.

vol% between 0.14–0.41 SBR and, for higher SBR, it exhibited a substantial reduction (Kibret et al., 2021). Fig. 3(b) shows a steady reduction of CO from 44.32 to 33.57 vol% for 0.5 and 1.2 SBR. CH_4 slightly reduce from 7.4 to 6.95 vol% for higher SBR. The observed reduction of CO_2 with growing SBR might be attributed to the Boudouard reaction (R_3) and CO_2 reforming reactions ($C_xH_y + x\,CO_2 \leftrightarrow 2x\,CO + (y/2)\,H_2$) promoted by CO_2 (Evaristo et al., 2021), furthering the increase of H_2 content.

Comparing both atmospheres for SCG gasification, the steam-enhanced medium provided higher H_2/CO with lower CO_2 vol%. When the interest is H_2-rich gas production from SCG gasification, results point out the medium of 0.18 CO_2BR and 1.2 SBR as the optimum conditions. On the other hand, 0.27 CO_2BR and 0.8 SBR provided a higher syngas yield and, consequently, better LHV_{syngas} and CGE, as discussed next.

Finally, Fig. 4(f) shows char and soot formed during the steam-enhanced experiments as a function of SBR. As expected (Evaristo et al., 2021), char formation decreased as the SBR increased. Differently from the CO_2-enhanced atmosphere, it is seen an increasing trend of soot quantity (mg. g_{SCG}^{-1}) when the SBR increases, with considerable higher values (10.53, 15.13 and 17.56 mg. g_{SCG}^{-1} for 0.5, 0.8, 1.2 SBR, respectively) compared to O_2/N_2 (8.51) and $O_2/CO_2/N_2$ (8.33, 7.98, 5.73 mg. g_{SCG}^{-1} for 0.09, 0.18, 0.27 CO_2BR) mediums.

3.3. Energy analysis

The effects of the CO_2BR and SBR gasification mediums on the LHV_{syngas} and CGE are shown in Figs. 4(a) and (b), respectively. Meanwhile, Table 5 shows the results for Q_{syngas} and CCE.

Table 5

XXXQ_{syngas} (Nm³. h⁻¹) and CCE (%) for O_2/N_2, CO_2BR (0.09, 0.18 and 0.27) and SBR (0.5, 0.8 and 1.2).

	Q_{syngas} [a]	CCE [b]
O_2		
0.0	0.075	138.39
CO_2BR		
0.09	0.074	139.45
0.18	0.073	126.75
0.27	0.084	154.54
SBR		
0.5	0.098	189.03
0.8	0.116	195.16
1.2	0.058	86.99

[a] Nm³. h⁻¹.
[b] %.

Fig. 4(a) shows that adding CO_2 to the gasification medium promoted a minor reduction of LHV_{syngas} compared to O_2/N_2, which could be due to the dilution of the CO_2 in the produced gas (Kibret et al., 2021). When increasing the CO_2BR, the LHV_{syngas} was augmented from 10.77–11.97 MJ. Nm³, according to the producer gas composition (higher H_2 and CO vol%). The LHV_{syngas} range and behavior are in line with (Kibret et al., 2021), which showed a slight reduction of heating value for lower CO_2 concentrations in gasification medium followed by an increasing trend for higher CO_2BR.

Fig. 4(b) shows the growing behavior of LHV_{syngas} from 10.80 MJ. Nm⁻³ (O_2/N_2 up to 12.10 MJ. Nm⁻³ when SBR raised from

Table 6

Chemical, physical and total H_2-exergy (Ex_{H_2}) values (in kJ. $kg_{biomass}^{-1}$) and H_2-exergy efficiency (η_{H_2} in %) for O_2/N_2, CO_2BR (0.09, 0.18 and 0.27) and SBR (0.5, 0.8 and 1.2).

Gasification medium		ex_{ch}[a]	ex_{ph}[a]	Ex_{H_2}[a]	η_{H_2}[b]
O_2	–	5.953	0.410	6.363	20.58
CO_2BR	0.09	6.097	0.420	12.881	21.07
	0.18	7.583	0.523	14.623	26.21
	0.27	8.251	0.569	16.926	28.52
SBR	0.5	7.730	0.533	17.083	26.71
	0.8	13.902	0.958	23.123	48.05
	1.2	8.555	0.590	24.005	29.57

[a] kJ. $kg_{biomass}^{-1}$.
[b] %.

0.5 to 1.2, following the producer gas composition. Results align with the previous research (Kibret et al., 2021), which reported a slightly lower heating value for CO_2 medium than the steam-enhanced during SCG gasification.

The calculated CGE and CCE (Table 5) depend on the Q_{syngas}, obtained experimentally. Even though the LHV_{syngas} of steam gasification enhanced due to H_2 and CO increasing (Fig. 3(a)), the Q_{syngas} slightly reduced between 0.09 and 0.18 CO_2BR (Table 5), resulting in a slight reduction of CGE (139.45 and 126.75%) compared to O_2/N_2 (141.07%).

The CGE for steam gasification reported higher values compared to CO_2 medium and an upward trend up to 0.8 SBR, followed by a pronounced reduction related to the Q_{syngas} (Table 5) when increasing SBR to 1.2. The maximum CGE and CCE were evidenced for 0.027 CO_2BR with 155 and 154% and 0.8 SBR with 210.7 and 195.16%, respectively.

3.4. Exergy analysis

H_2-exergy (Ex_{H_2}) (Fig. 4(c)) and H_2-exergy efficiency (η_{H_2}) (Fig. 4(d)) provides a reliable performance indicator for H_2-rich gas production. Compared to O_2/N_2 medium, the Ex_{H_2} was higher when gasifying with a steam/CO_2 enhanced environment, with superior values reported for higher SBR (0.8 and 1.2). Results ranges align with previous SCG research (Evaristo et al., 2021) and other biomass residues (Zhang et al., 2019b). In addition, the obtained upward trend for Ex_{H_2} and η_{H_2} with CO_2Br increase aligns with the previous study that reported a similar behavior for rice straw biomass (Parvez et al., 2016).

The Ex_{H_2} and η_{H_2} of CO_2-enhanced gasification increased compared to O_2/N_2, supporting a past study that reported an H_2 exergy increase with increasing CO_2BR in gasification medium for different biomass feedstocks (Parvez et al., 2016). Even though the H_2 yield (vol%) presented a maximum value for 0.18 CO_2Br and a reduction when increasing the CO_2BR to 0.27 (Fig. 3(a)), the Q_{syngas} (Table 6) was higher for 0.27 CO_2BR, resulting in a higher H_2 production in mol. $kg_{biomass}^{-1}$ and a greater Ex_{H_2}.

Regarding steam-enhanced gasification, the Ex_{H_2} (Fig. 3(b)) increased 29.79% for 0.5 SBR compared to O_2/N_2. The increasing H_2-exergy production might be attributed to the H_2 yield growths, which can be fundamentally associated with the fact that more moisture content at high gasification temperatures boosted the steam reforming reactions (He et al., 2009). As expected, the resulting growth in the H_2 yield during Steam-enhanced gasification led to greater exergy of produced H_2 and consequently to a higher η_{H_2}.

The maximum efficiency considering all investigated atmospheres was attempted for 0.8 SBR with a η_{H_2} of 48.05%. When increasing the SBR to 1.2, a reduction to 29.07% was evidenced. This behavior might be related to the excessive low-temperature steam reduced reaction temperature (Wang et al., 2012). The described behavior for Steam-enhanced gasification, where a critical SBR (generally between 0.70 and 3.41 depending on feedstock and process parameters) is obtained, followed by a reduction of η_{H_2} with SBR further increasing, aligns with previous literature (Zhang et al., 2019b).

The initial increases in η_{H_2} might be related to a higher amount of moisture content and, consequently, the promotion of a superior mixing with the other materials endorsed by the higher steam flow, favoring the hydrocarbon cracking reaction ($C_nH_m + 2n\,H_2O \rightarrow n\,CO_2 + (2n + m/2)\,H_2$) (Li et al., 2014), water-gas-shift reaction (R_5), char-reforming (R_4) (Wu et al., 2018) and methane-steam-reforming reaction (R_7) (Li et al., 2014). The downward trend observed for higher SBR might be attributed to the insufficient char considering the injected steam and the decreasing gas residence time within the reaction chamber, promoted by the growing steam flow rate (Chuayboon et al., 2018; Li et al., 2014). In summary, results indicate that SCG reported encouraging Ex_{H_2} and η_{H_2} for hydrogen production.

4. Conclusion

The steam/CO_2-enhanced gasification of SCG (clean energy carrier) focusing on hydrogen production can be seen as a commitment to waste mitigation strategies and renewable energy sources. This work investigated the effects of CO_2BR and SBR on energy and exergy performance, focusing on hydrogen production. The following conclusions have been drawn:

i) As a strategy for carbon capture and usage, maximum H_2 yield was obtained for 0.18 CO_2BR. Nevertheless, the H_2-exergy production and efficiency were higher for 0.27 CO_2BR due to higher syngas yield. Therefore, adding CO_2 to the gasification medium promotes its utilization in carbon capture systems, enhancing H_2 exergy efficiency and reducing soot formation.

ii) For 1000 °C gasification, an optimum steam flow rate (0.8 SBR) was identified, resulting in a maximum H_2 yield production and consequently higher H_2-exergy and η_{H_2} for the SCG feedstock. The hydrogen yield declined when the steam flow was further increased.

iii) The steam-enhanced medium provided higher H_2/CO with lower CO_2 vol%. When the interest is H_2-rich gas production from SCG gasification, results point out the medium of 0.18 CO_2BR and 1.2 SBR as the optimum conditions. On the other hand, 0.27 CO_2BR and 0.8 SBR provided a higher syngas yield and, consequently, better LHV_{syngas} and CGE.

Considering its low pollution characteristics and zero carbon emission, hydrogen research has been widely promoted and is most likely the world's long-term alternative fuel. Furthermore, the steam/CO_2-enhanced gasification results showed suitability as a valuation route for promoting WTH production and might encourage the development and further use of lignocellulosic waste as cleaner energy sources. Future works will approach other temperature ranges, different urban waste sources and torrefaction as pre-treatment for gasification (Macedo et al., 2022; Silveira et al., 2021a, 2021b). In addition, further research will be conducted on the exergoenvironmental and exergoeconomics aspects.

Declaration of Competing Interests

The authors declare that they have no known competing financial interests or personal relationships that could have appeared to influence the work reported in this paper.

CRediT authorship contribution statement

Juliana Petrocchi Rodrigues: Formal analysis, Investigation. **Grace F. Ghesti:** Conceptualization, Funding acquisition, Investigation, Formal analysis, Writing – original draft. **Edgar A. Silveira:** Conceptualization, Formal analysis, Writing – original draft. **Giulia Cruz Lamas:** Formal analysis, Writing – original draft. **Ricardo Ferreira:** Formal analysis, Investigation, Writing – review & editing. **M. Costa:** Conceptualization, Methodology, Resources, Supervision, Project administration.

Data Availability

Data will be made available on request.

Acknowledgments

References

Adánez-Rubio, I., Ferreira, R., Rio, T., Alzueta, M.U., Costa, M., 2020. Soot and char formation in the gasification of pig manure in a drop tube reactor. Fuel 281, 118738. doi:10.1016/j.fuel.2020.118738.

Anniwaer, A., Chaihad, N., Zhang, M., Wang, C., Yu, T., Kasai, Y., Abudula, A., Guan, G., 2021. Hydrogen-rich gas production from steam co-gasification of banana peel with agricultural residues and woody biomass. Waste Manag. 125, 204–214. doi:10.1016/j.wasman.2021.02.042.

Ashik, U.P.M., Wan Daud, W.M.A., Abbas, H.F., 2015. Production of greenhouse gas free hydrogen by thermocatalytic decomposition of methane - A review. Renew. Sustain. Energy Rev. 44, 221–256. doi:10.1016/j.rser.2014.12.025.

Atabani, A.E., Ali, I., Naqvi, S.R., Badruddin, I.A., Aslam, M., Mahmoud, E., Almomani, F., Juchelková, D., Atelge, M.R., Khan, T.M.Y., 2022a. A state-of-the-art review on spent coffee ground (SCG) pyrolysis for future biorefinery. Chemosphere 286, 131730. doi:10.1016/j.chemosphere.2021.131730.

Atabani, A.E., Mahmoud, E., Aslam, M., Naqvi, S.R., Juchelková, D., Bhatia, S.K., Badruddin, I.A., Khan, T.M.Y., Hoang, A.T., Palacky, P., 2022b. Emerging Potential of Spent Coffee Ground Valorization For Fuel Pellet Production in a biorefinery, Environment, Development and Sustainability. Springer, Netherlands doi:10.1007/s10668-022-02361-z.

Bach, Q.V., Nguyen, D.D., Lee, C.J., 2019. Effect of torrefaction on steam gasification of biomass in dual fluidized bed reactor—a process simulation study. Bioenergy Res 12, 1042–1051. doi:10.1007/s12155-019-10011-y.

Butterman, H.C., Castaldi, M.J., 2007. Influence of CO2 injection on biomass gasification. Ind. Eng. Chem. Res. 46, 8875–8886. doi:10.1021/ie071160n.

Cay, H., Duman, G., Yanik, J., 2019. Two-step gasification of biochar for hydrogen-rich gas production: effect of the biochar type and catalyst. Energy and Fuels 33, 7398–7405. doi:10.1021/acs.energyfuels.9b01354.

Chaiklangmuang, S., Kurosawa, K., Li, L., Morishita, K., Takarada, T., 2015. Thermal degradation behavior of coffee residue in comparison with biomasses and its product yields from gasification. J. Energy Inst. 88, 323–331. doi:10.1016/j.joei.2014.08.001.

Chen, W.H., Chen, C.J., Hung, C.I., Shen, C.H., Hsu, H.W., 2013. A comparison of gasification phenomena among raw biomass, torrefied biomass and coal in an entrained-flow reactor. Appl. Energy 112, 421–430. doi:10.1016/j.apenergy.2013.01.034.

Chuayboon, S., Abanades, S., Rodat, S., 2018. Experimental analysis of continuous steam gasification of wood biomass for syngas production in a high-temperature particle-fed solar reactor. Chem. Eng. Process. Process Intensif. 125, 253–265. doi:10.1016/j.cep.2018.02.004.

Colantoni, A., Paris, E., Bianchini, L., Ferri, S., Marcantonio, V., Carnevale, M., Palma, A., Civitarese, V., Gallucci, F., 2021. Spent coffee ground characterization, pelletization test and emissions assessment in the combustion process. Sci. Rep. 11, 1–14. doi:10.1038/s41598-021-84772-y.

Costa, F.C., Santanna, M.S., S. Chaves, B., Silveira, E.A., 2021. Hybridization of energy sources as an energy alternative. 26th International Congress of Mechanical Engineering COBEM.

Couto, N., Silva, V., Monteiro, E., Brito, P.S.D., Rouboa, A., 2013. Experimental and numerical analysis of coffee husks biomass gasification in a fluidized bed reactor. Energy Procedia 36, 591–595. doi:10.1016/j.egypro.2013.07.067.

Cséfalvay, E., Horváth, I.T., 2018. Sustainability assessment of renewable energy in the United States, Canada, the European Union, China, and the Russian Federation. ACS Sustain. Chem. Eng. 6, 8868–8874. doi:10.1021/acssuschemeng.8b01213.

Dang, C.H., Nguyen, T.D., 2019. Physicochemical characterization of robusta spent coffee ground oil for biodiesel manufacturing. Waste and Biomass Valorization 10, 2703–2712. doi:10.1007/s12649-018-0287-9.

de Oliveira, J.L., da Silva, J.N., Martins, M.A., Pereira, E.G., da Conceição Trindade Bezerra e Oliveira, M., 2018. Gasification of waste from coffee and eucalyptus production as an alternative source of bioenergy in Brazil. Sustain. Energy Technol. Assessments 27, 159–166. doi:10.1016/j.seta.2018.04.005.

Detchusananard, T., Im-orb, K., Ponpesh, P., Arpornwichanop, A., 2018. Biomass gasification integrated with CO2 capture processes for high-purity hydrogen production: process performance and energy analysis. Energy Convers. Manag. 171, 1560–1572. doi:10.1016/j.enconman.2018.06.072.

Deutsch, L., Lamas, G.C., Pereira, T.S., Silveira, E.A., Caldeira-Pires, A., 2022. Life cycle and risk assessment of vinasse storage dams: a Brazilian sugar-energy refinery analysis. Sustain. Futur. 4, 100083. doi:10.1016/j.sftr.2022.100083.

Efthymiopoulos, I., Hellier, P., Ladommatos, N., Kay, A., Mills-Lamptey, B., 2018. Integrated strategies for water removal and lipid extraction from coffee industry residues. Sustain. Energy Technol. Assessments 29, 26–35. doi:10.1016/j.seta.2018.06.016.

Evaristo, R.B.W., Ferreira, R., Petrocchi Rodrigues, J., Ghesti, G.F., Silveira, E.A., Costa, M., 2021. Multiparameter-analysis of CO2/Steam-enhanced gasification and pyrolysis for syngas and biochar production from low-cost feedstock. Energy Convers. Manag. X 12, 100138. doi:10.1016/j.ecmx.2021.100138.

Farooq, A., Rhee, G.H., Lee, I.-Khan, M.A., Lee, S.H., Jung, S.-C., Jeon, B.-H., Chen, W.-H., Park, Y.-K., 2021. Waste furniture gasification using rice husk based char catalysts for enhanced hydrogen generation. Bioresour. Technol. 341, 125813. doi:10.1016/j.biortech.2021.125813.

Ferreira, R., Petrova, T., Pereira, A.F., Costa, M., Inaydenova, I., Atanasova-Vladimirova, S., Ranguelov, B., 2021. Size-segregated particulate matter from gasification of bulgarian agro-forest biomass residue. Energies 14, 385. doi:10.3390/en14020385.

Ferreiro, A.I., Segurado, R., Costa, M., 2020. Modelling soot formation during biomass gasification. Renew. Sustain. Energy Rev. 134, 110380. doi:10.1016/j.rser.2020.110380.

Galvão, L.G.O.B.S.C., Morais, M.V.G.de, Vale, A.T.do V., Caldeira-Pires, A., Rousset, P., Silveira, E.A., 2020. Combined thermo-acoustic upgrading of solid fuel: experimental and numerical investigation. In: 28th Eur. Biomass Conf. Exhib., pp. 6–9. doi:10.5071/28thEUBCE2020-3DO.6.2.

George, J., Arun, P., Muraleedharan, C., 2019. Experimental investigation on co-gasification of coffee husk and sawdust in a bubbling fluidised bed gasifier. J. Energy Inst. 92, 1977–1986. doi:10.1016/j.joei.2018.10.014.

Ghesti, G.F., Silveira, E.A., Guimarães, M.G., Evaristo, R.B.W., Costa, M., 2022. Towards a sustainable waste-to-energy pathway to pequi biomass residues: Biochar, syngas, and biodiesel analysis. Waste Manag. 143, 144–156. doi:10.1016/j.wasman.2022.02.022.

He, M., Xiao, B., Liu, S., Guo, X., Luo, S., Xu, Z., Feng, Y., Hu, Z., 2009. Hydrogen-rich gas from catalytic steam gasification of municipal solid waste (MSW): Influence of steam to MSW ratios and weight hourly space velocity on gas production and composition. Int. J. Hydrogen Energy 34, 2174–2183. doi:10.1016/j.ijhydene.2008.11.115.

Hu, Y., Pang, K., Cai, L., Liu, Z., 2021. A multi-stage co-gasification system of biomass and municipal solid waste (MSW) for high quality syngas production. Energy 221, 119639. doi:10.1016/j.energy.2020.119639.

Inayat, A., Khan, Z., Aslam, M., Shahbaz, M., Ahmad, M.M., Abdul Mutalib, M.I., Yusup, S., 2020. Integrated adsorption steam gasification for enhanced hydrogen production from palm waste at bench scale plant. Int. J. Hydrogen Energy. doi:10.1016/j.ijhydene.2020.12.008.

Ismail, T.M., Abd El-Salam, M., Monteiro, E., Rouboa, A., 2016. Eulerian - Eulerian CFD model on fluidized bed gasifier using coffee husks as fuel. Appl. Therm. Eng. 106, 1391–1402. doi:10.1016/j.applthermaleng.2016.06.102.

Kibret, H.A., Kuo, Y.-L., Ke, T.-Y., Tseng, Y.-H., 2021. Gasification of spent coffee grounds in a semi-fluidized bed reactor using steam and CO2 gasification medium. J. Taiwan Inst. Chem. Eng. 119, 115–127. doi:10.1016/j.jtice.2021.01.029.

Lamas, G.C., Costa, F.C., Santanna, M.S., S. Chaves, B., Galvão, L.G.O., Macedo, L., Pires, A.C.-, Silveira, E.A., 2022. Steam-enhanced gasification of a hybrid blend composed of municipal solid waste and torrefied biomass. In: 30th EUROPEAN BIOMASS CONFERENCE AND EXHIBITION PROCEEDINGS, pp. 9–12. doi:10.5071/30thEUBCE2022-1CV.2.2 (ISSN 2282-5819).

Li, W., Li, Q., Chen, R., Wu, Y., Zhang, Y., 2014. Investigation of hydrogen production using wood pellets gasification with steam at high temperature over 800 °c to 1435 °c. Int. J. Hydrogen Energy 39, 5580–5588. doi:10.1016/j.ijhydene.2014.01.102.

Macedo, L.A., Silveira, E.A., Rousset, P., Valette, J., Commandré, J.-M., 2022. Synergistic effect of biomass potassium content and oxidative atmosphere: Impact on torrefaction severity and released condensables. Energy 254, 124472. doi:10.1016/j.energy.2022.124472.

McNutt, J., He, Q.(Sophia), 2019. Spent coffee grounds: a review on current utilization. J. Ind. Eng. Chem. 71, 78–88. doi:10.1016/j.jiec.2018.11.054.

Mendoza Martinez, C.L., Saari, J., Melo, Y., Cardoso, M., de Almeida, G.M., Vakkilainen, E., 2021a. Evaluation of thermochemical routes for the valorization of solid coffee residues to produce biofuels: a Brazilian case. Renew. Sustain. Energy Rev. 137, 110585. doi:10.1016/j.rser.2020.110585.

Mendoza Martinez, C.L., Saari, J., Melo, Y., Cardoso, M., de Almeida, G.M., Vakkilainen, E., 2021b. Evaluation of thermochemical routes for the valorization of solid coffee residues to produce biofuels: a Brazilian case. Renew. Sustain. Energy Rev. 137, 110585. doi:10.1016/j.rser.2020.110585.

Menezes, L.N.B., Silveira, E.A., Mazzoni, J.V.S., Evaristo, R.B.W., Rodrigues, J.S., Lamas, G.C., Suarez, P.A.Z., Ghesti, G.F., 2022. Alternative valuation pathways for primary, secondary, and tertiary sewage sludge: biochar and bio-oil production for sustainable energy. Biomass Convers. Biorefinery. doi:10.1007/s13399-022-02543-9.

Midilli, A., Kucuk, H., Topal, M.E., Akbulut, U., Dincer, I., 2021. A comprehensive review on hydrogen production from coal gasification: Challenges and Opportunities. Int. J. Hydrogen Energy 46, 25385–25412. doi:10.1016/j.ijhydene.2021.05.088.

Miranda, M.R., da, S., Veras, C.A.G., Ghesti, G.F., 2020. Charcoal production from waste pequi seeds for heat and power generation. Waste Manag 103, 177–186. doi:10.1016/j.wasman.2019.12.025.

Moreira, R., Bimbela, F., Gil-Lalaguna, N., Sánchez, J.L., Portugal, A., 2021. Clean syngas production by gasification of lignocellulosic char: State of the art and future prospects. J. Ind. Eng. Chem. 101, 1–20. doi:10.1016/j.jiec.2021.05.040.

Pacioni, T.R., Soares, D., Di Domenico, M., Alves, J.L.F., Virmond, E., Moreira, R., de, F.P.M., José, H.J., 2021. Kinetic modeling of CO2 gasification of biochars prepared from Brazilian agro-industrial residues: effect of biomass indigenous mineral content. Biomass Convers. Biorefinery. doi:10.1007/s13399-021-01671-y.

Pacioni, T.R., Soares, D., Domenico, M.Di, Rosa, M.F., Moreira, R.de F.P.M., José, H.J., 2016. Bio-syngas production from agro-industrial biomass residues by steam gasification. Waste Manag. 58, 221–229. doi:10.1016/j.wasman.2016.08.021.

Parascanu, M.M., Sandoval-Salas, F., Soreanu, G., Valverde, J.L., Sanchez-Silva, L., 2017. Valorization of Mexican biomasses through pyrolysis, combustion and gasification processes. Renew. Sustain. Energy Rev. 71, 509–522. doi:10.1016/j.rser.2016.12.079.

Parvez, A.M., Mujtaba, I.M., Wu, T., 2016. Energy, exergy and environmental analyses of conventional, steam and CO2-enhanced rice straw gasification. Energy 94, 579–588. doi:10.1016/j.energy.2015.11.022.

Prasertcharoensuk, P., Bull, S.J., Arpornwichanop, A., Phan, A.N., 2021. Sustainable hydrogen production from waste wood and CO2. Ind. Eng. Chem. Res. 60, 12362–12376. doi:10.1021/acs.iecr.1c01810.

Qin, W., Luo, L., Chen, S., Iqbal, T., Xiao, X., Dong, C., 2021. Efficient strategy of utilizing alkaline liquid waste boosting biomass chemical looping gasification to produce hydrogen. Fuel Process. Technol. 217, 106818. doi:10.1016/j.fuproc.2021.106818.

Rajesh Banu, J., Yukesh Kannah, R., Dinesh Kumar, M., Preethi, Kavitha, S., Gunasekaran, M., Zhen, G., Awasthi, M.K., Kumar, G., 2021. Spent coffee grounds based circular bioeconomy: Technoeconomic and commercialization aspects. Renew. Sustain. Energy Rev. 152, 111721. doi:10.1016/j.rser.2021.111721.

Reyes, L., Abdelouahed, L., Campusano, B., Buvat, J.C., Taouk, B., 2021. Exergetic study of beech wood gasification in fluidized bed reactor using CO2 or steam as gasification agents. Fuel Process. Technol. 213, 106664. doi:10.1016/j.fuproc.2020.106664.

Santanna, M.S., Silveira, E.A., Caldeira-Pires, A., 2021. Thermochemical pathways for municipal lignocellulosic waste as biofuel. 29th European Biomass Conference and Exhibition doi:10.5071/29thEUBCE2021-3DV.6.8.

Santanna, M.S., Silveira, E.A., Macedo, L., Galvão, L.G.O., Caldeira-Pires, A., 2020. Torrefaction of lignocellulosic municipal solid waste: thermal upgrade for energy use. In: 28th European Biomass Conference and Exhibition. Marseille, pp. 188–191. doi:10.5071/28thEUBCE2020-1DV.1.34.

Silveira, E.A., Luz, S., Candelier, K., Macedo, L.A., Rousset, P., 2021a. An assessment of biomass torrefaction severity indexes. Fuel 288, 119631. doi:10.1016/j.fuel.2020.119631.

Silveira, E.A., Macedo, L.A., Candelier, K., Rousset, P., Commandré, J.-M., 2021b. Assessment of catalytic torrefaction promoted by biomass potassium impregnation through performance indexes. Fuel 304, 121353. doi:10.1016/j.fuel.2021.121353.

Silveira, E.A., Macedo, L.A., Rousset, P., Candelier, K., Galvão, L.G.O., Chaves, B.S., Commandré, J.-M., 2022a. A potassium responsive numerical path to model catalytic torrefaction kinetics. Energy 239, 122208. doi:10.1016/j.energy.2021.122208.

Silveira, E.A., S., Chaves, B., Macedo, L.A., Ghesti, G.F., Evaristo, R.B.W., Cruz Lamas, G., Luz, S.M., Protásio, T., Rousset, P., 2022b. A hybrid optimization approach towards energy recovery from torrefied waste blends. SSRN Electron. J. doi:10.2139/ssrn.4217358.

Silveira, E.A., Santanna, M.S., Barbosa Souto, N.P., Lamas, G.C., Galvão, L.G.O., Luz, S.M., Caldeira-Pires, A., 2022c. Urban lignocellulosic waste as biofuel: thermal improvement and torrefaction kinetics. J. Therm. Anal. Calorim. doi:10.1007/s10973-022-11515-0.

Tang, F., Chi, Y., Jin, Y., Zhu, Z., Ma, J., 2022. Gasification characteristics of a simulated waste under separate and mixed atmospheres of steam and CO2. Fuel 317, 123527. doi:10.1016/j.fuel.2022.123527.

Torres, C., Urvina, L., de Lasa, H., 2019. A chemical equilibrium model for biomass gasification. Application to Costa Rican coffee pulp transformation unit. Biomass Bioenergy 123, 89–103. doi:10.1016/j.biombioe.2019.01.025.

Vikram, S., Rosha, P., Kumar, S., Mahajani, S., 2022. Thermodynamic analysis and parametric optimization of steam-CO2 based biomass gasification system using Aspen PLUS. Energy 241, 122854. doi:10.1016/j.energy.2021.122854.

Waldheim, L., Nilsson, T., 2001. Heating value of gases from report prepared for: IEA bioenergy agreement. English.

Wang, C., Li, L., Chen, Y., Ge, Z., Jin, H., 2021. Supercritical water gasification of wheat straw: composition of reaction products and kinetic study. Energy 227, 120449. doi:10.1016/j.energy.2021.120449.

Wang, J., Cheng, G., You, Y., Xiao, B., Liu, S., He, P., Guo, D., Guo, X., Zhang, G., 2012. Hydrogen-rich gas production by steam gasification of municipal solid waste (MSW) using NiO supported on modified dolomite. Int. J. Hydrogen Energy 37, 6503–6510. doi:10.1016/j.ijhydene.2012.01.070.

Wijayasekera, S.C., Hewage, K., Siddiqui, O., Hettiaratchi, P., Sadiq, R., 2022. Waste-to-hydrogen technologies: a critical review of techno-economic and socio-environmental sustainability. Int. J. Hydrogen Energy 47, 5842–5870. doi:10.1016/j.ijhydene.2021.11.226.

Wu, Y., Liao, Y., Liu, G., Ma, X., 2018. Syngas production by chemical looping gasification of biomass with steam and CaO additive. Int. J. Hydrogen Energy 43, 19375–19383. doi:10.1016/j.ijhydene.2018.08.197.

Xiang, X., Gong, G., Wang, C., Cai, N., Zhou, X., Li, Y., 2021. Exergy analysis of updraft and downdraft fixed bed gasification of village-level solid waste. Int. J. Hydrogen Energy 46, 221–233. doi:10.1016/j.ijhydene.2020.09.247.

Zhang, Y., Li, B., Li, H., Zhang, B., 2012. Exergy analysis of biomass utilization via steam gasification and partial oxidation. Thermochim. Acta 538, 21–28. doi:10.1016/j.tca.2012.03.013.

Zhang, Y., Li, L., Xu, P., Liu, B., Shuai, Y., Li, B., 2019a. Hydrogen production through biomass gasification in supercritical water: A review from exergy aspect. Int. J. Hydrogen Energy 44, 15727–15736. doi:10.1016/j.ijhydene.2019.01.151.

Zhang, Y., Xu, P., Liang, S., Liu, B., Shuai, Y., Li, B., 2019b. Exergy analysis of hydrogen production from steam gasification of biomass: A review. Int. J. Hydrogen Energy 44, 14290–14302. doi:10.1016/j.ijhydene.2019.02.064.

Zhang, Y., Zhao, Y., Gao, X., Li, B., Huang, J., 2015. Energy and exergy analyses of syngas produced from rice husk gasification in an entrained flow reactor. J. Clean. Prod. 95, 273–280. doi:10.1016/j.jclepro.2015.02.053.